

Saturable absorption, wave mixing, and phase conjugation with bacteriorhodopsin

Ofer Werner and Baruch Fischer

Department of Electrical Engineering, Technion—Israel Institute of Technology, Haifa 32000, Israel

Aaron Lewis

Department of Applied Physics, The Hebrew University, Jerusalem, Israel

Isaiah Nebenzahl

Racah Institute of Physics, The Hebrew University, Jerusalem, Israel

Received February 7, 1990; accepted July 1, 1990

Bacteriorhodopsin exhibits strong nonlinear and saturation behavior with very low light intensities (~ 10 mW/cm²). A model and an experimental study of the saturation are described. Four-wave mixing experiments are used for obtaining phase conjugation and information on the holographic resolution of the material. Two kinds of samples were prepared and used in the experiments: films of bacteriorhodopsin in a solid polyvinylalcohol (polymer) matrix and in water.

With the rapid growth of photonics technology, considerable effort is being directed toward the development of new materials. Better materials are still needed for the implementation of ideas and devices such as spatial light modulators and switches. The search has already encompassed several kinds of material, including unusual organic materials and even bacterial membranes,^{1–5} which have been used for second-harmonic generation, dynamic holography, and other purposes. The active nonlinear component in these bacterial membranes is a protein called bacteriorhodopsin (BR). BR was recently considered for use as an optic switch⁶ for information-recording purposes^{2,5,7} and neural networks.⁸ A Soviet group^{3,4} has done an intensive study of BR. Among many results, they reported on dynamic holography and light-induced dichroism. In this Letter we present a study of the nonlinear and saturation properties of BR. For these measurements we used BR-doped polymer films and BR suspensions in water. A model for the saturation behavior is described and compared with experimental results. We also present four-wave mixing and phase-conjugation experiments and study the resolution and efficiency of the samples.

BR is contained in the purple membrane of the bacterium *Halobacterium halobium*. It is a light-driven proton pump and is related to the visual pigment rhodopsin, having a strong absorption in a broad region of the visible spectrum. By absorbing light the molecule undergoes several structural transformations in a well-defined photocycle.⁹ We are interested only in several states in this photocycle, which are described in the simplified level diagram of Fig. 1. The basic BR state is transformed to an *M* state through the short-lived intermediates *K* and *L* (not shown in figure) by absorbing photons in the BR absorption band, which has a peak at 570 nm. The

lifetime of the *M* state, denoted τ , is dependent on the relative humidity and the pH of the environment in which the membranes are suspended.^{10,11} This time constant at room temperature can be varied from a few milliseconds for high-humidity samples to hours in samples that are dry and are at a high pH. Alternatively, light within the 412-nm *M* absorption band converts the *M* state into BR in 200 nsec (Fig. 1). It should be emphasized that the above two light-induced transitions are unidirectional. Thus, the 570-nm photons do not induce the reverse transitions *M* → BR, and the 412-nm light does not contribute directly to the BR → *M* transition. We also note that the two absorption bands centered near 570 and 412 nm are broad, with a width of ~ 100 nm, and have a small but nonvanishing overlap. This is significant in our study below, in which we take into account the possibility of simultaneously having finite absorption cross sections for both transitions.

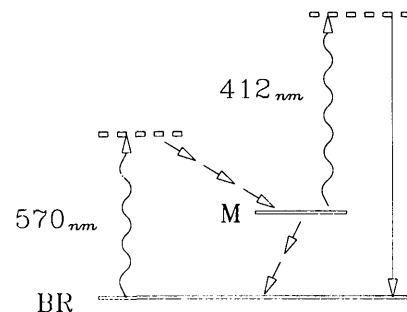


Fig. 1. Simplified diagram of the BR photocycle. The transition BR → *M* can be induced by 570 ± 75 -nm photons through short-lived intermediates. The *M* → BR thermal lifetime is τ , but this transition can be induced photochemically by 412 ± 75 -nm photons.

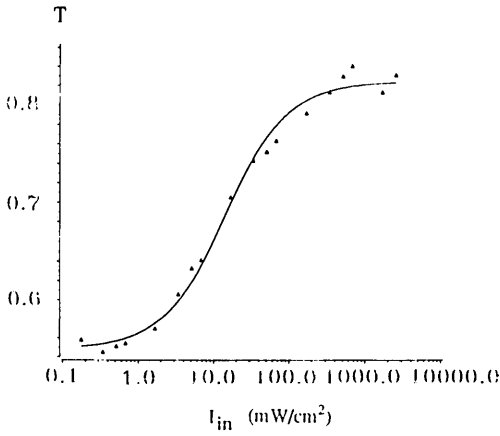


Fig. 2. Transmissivity measurements (triangles) of the solid BR-PVA sample no. 1 as a function of the input-beam intensity (by varying the input) for a wavelength of 514.5 nm. The solid curve describes the theoretical results, with the parameters given in the text.

Although BR is a stable material, there are still difficulties in preparing samples with good optical quality. Following the technique developed by Chen *et al.*,² we prepared solid BR-doped polymer films. Films with a thickness of $\sim 300 \mu\text{m}$ were obtained. We also studied liquid samples of BR suspensions in pure water. The thickness of these samples was $\sim 100 \mu\text{m}$.

The above description of the BR states permits the use of the rate-equation approximation for the population of the levels BR and M . It gives the absorption behavior of the system and is found to describe remarkably the saturation experiments below. The rate equation for the level populations (denoted by B and M per unit volume for the BR and M levels, respectively) is,

$$\frac{dM}{dt} = \sigma_1 \bar{I} B - \frac{M}{\tau} - \sigma_2 \bar{I} M, \quad (1)$$

where $\bar{I} = I/h\nu$ is the photon density flux of the light beam, I is the intensity, and ν is the frequency. σ_i are the absorption cross sections for the (nonradiative) transitions $\text{BR} \rightarrow M$ and $M \rightarrow \text{BR}$ that depend on the wavelength of the light beam. τ is the relaxation time for the transition $M \rightarrow \text{BR}$, which is relatively long. The steady-state solution of Eq. (1) gives the following populations,

$$B = N \left[\frac{1 + \sigma_2 \tau \bar{I}}{1 + (\sigma_1 + \sigma_2) \tau \bar{I}} \right], \quad (2)$$

$$M = N - B,$$

where N is the active (light-adapted) density of BR molecules. Then the exponential absorption constant is given by

$$\alpha = N \sigma_1 \left[\frac{1 + 2\sigma_2 \tau \bar{I}}{1 + (\sigma_1 + \sigma_2) \tau \bar{I}} \right] = \alpha_0 - \frac{gI}{1 + I/I_S}, \quad (3)$$

where $\alpha_0 = N\sigma_1$, $g = N\sigma_1(\sigma_1 - \sigma_2)\tau/h\nu$, and $I_S = h\nu/(\sigma_1 + \sigma_2)\tau$ (the saturation intensity parameter).

For light with wavelength of $\sim 570 \text{ nm}$ and above, $\sigma_1 \gg \sigma_2$ and $\alpha(I)$ behaves as a regular saturable absorber. For wavelengths closer to 412 nm, $\sigma_2 > \sigma_1$ and the medium will have increasing absorption for increasing light intensities. Interesting behavior can also be obtained by using two wavelengths of approximately 570 and 412 nm simultaneously. We also note that the measured α contains absorption from other sources (such as linear absorption and scattering of the matrix) that can be included in the linear term α_0 in Eq. (3).

In the first experiments we studied the saturation properties of the samples. We measured the dependence of the absorption on the input-beam intensity. We used the 514.5-nm line of an argon-ion laser and the 632.8-nm wavelength of a He-Ne laser. The results are given in Fig. 2, which shows the transmissivity measurements (the triangles), corrected for Fresnel reflections, as a function of the input-beam intensity. We fitted a theoretical curve of the transmissivity (the solid curve) by using Eq. (3) and

$$\frac{dI}{dz} = -\alpha(I)I. \quad (4)$$

Since the intensity is varying along the beam propagation in the medium for a given input intensity, the exponential absorption constant $\alpha(I)$ is not constant, and thus we have had to extract the fitting parameters numerically. The theoretical curve closely follows the experimental results. The fitting parameters for our samples are given in Table 1. The difference in the nonlinear coefficients and the saturation constants of the samples are simply explained by the difference in the time constants (τ_i of sample i in Table 1) and the concentrations (N_i) of the samples. The ratios of the time constants and the BR concentrations in two samples can be obtained from the theoretical equalities

$$\frac{I_S^i}{I_S^j} = \frac{\tau_j}{\tau_i}, \quad \frac{g_i}{g_j} = \frac{N_i \tau_i}{N_j \tau_j}, \quad (5)$$

for parameters taken at the same wavelengths (then the σ_i are the same for the samples). Thus we can find the ratios of the time constants and the active concen-

Table 1. Fitting Parameters of Our Samples

No.	Sample	Wavelength (nm)	α_0 (cm ⁻¹)	I_S (mW/cm ²)	g (cm/mW)
1	BR-PVA	514.5	17.2	9.5	1.23
2	BR-PVA	514.5	17.9	36.1	0.29
3	BR in water	514.5	34.9	357.7	0.05
4	BR-PVA	632.8	8.2	4.1	0.83
5	BR-PVA	632.8	8.4	35.2	0.08

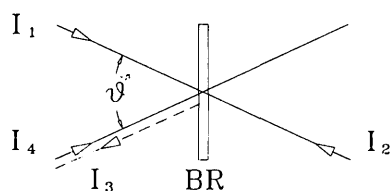


Fig. 3. Four-wave mixing configuration.



Fig. 4. Photograph of the diffracted phase-conjugate image carried by beam 3.

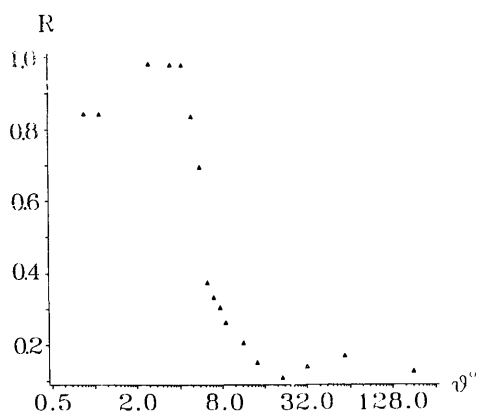


Fig. 5. Phase-conjugate reflectivity R (in arbitrary units) as a function of the angle ϕ for the liquid sample. The intensities in this experiment were $I_1 = I_4 = 370 \text{ mW/cm}^2$ and $I_2 = 863 \text{ mW/cm}^2$. The reflectivity of the solid (BR-PVA) slide was almost independent of the angle (it depends, however, on the beams' intensities).

trations for the samples. For example, from the data taken at 514.5 nm, we have $\tau_i/\tau_3 \approx 37.6, 9.9$ and $N_i/N_3 \approx 0.65, 0.58$ for samples $i = 1, 2$, respectively. Thus $N_1/N_2 \approx 1$. For 632.8 nm, $\tau_4/\tau_5 \approx 8.7$ and $N_4/N_5 \approx 1.2$. It is not surprising that the active concentration for all solid BR-PVA samples is almost the same. In fact, the different measurements of the BR-PVA were taken from the same slide with slightly different environments (humidity and location on the slide). For the decay time τ of level M , the liquid sample, which has the highest relative humidity, is known to be in the millisecond region. The solid BR-PVA decay time (without light) is longer and falls within 10–50 msec. For films that have increasingly less humidity, we can obtain longer τ and stronger nonlinearities.

We next studied four-wave mixing experiments with the BR samples. The configuration is shown in Fig. 3. Signal beam 4 has an angle of ϕ with the two counterpropagating pump beams 1 and 2. Only beams 1 and 4 are mutually coherent and write grat-

ings on the BR sample. We used the 514.5-nm line of the argon laser. Diffracted beam 3 is the phase conjugate of signal beam 4, and is shown in Fig. 4.

To obtain information on the resolution of the samples, we measured the reflectivity of the phase-conjugate signal as a function of the angle ϕ (inside the samples) between the signal and the pumps. In this experiment the intensities of the input beams were left unchanged. The reflectivity was $\sim 0.1\%$ and is dependent on the beams' intensities. By changing the angle, the grating period $\lambda_g = \lambda/[2n \sin(\phi/2)]$, where n is the refractive index of the slide, varies from tens of micrometers (for transmission gratings and low ϕ) to $\lambda/2n$ for $\phi \rightarrow 180^\circ$ (reflection gratings). Thus we were able to detect the ability to form a grating of that resolution in the BR samples. Figure 5 shows the measurements for the liquid sample. It can be seen that as ϕ exceeds 4.6° (corresponding to $\lambda_g = 4.6 \mu\text{m}$), the reflectivity drops and reaches a constant value at $\phi \approx 9.2^\circ$ ($\lambda_g \approx 2.3 \mu\text{m}$) of approximately one seventh of the low- ϕ value. In the solid slide, however, there is no ϕ dependence. This means that the resolution of the solid slide is at least $\lambda/2n = 0.17 \mu\text{m}$. On the other hand, the resolution of the liquid sample is limited to $\sim 4.6 \mu\text{m}$. We think that this limitation results from the random thermal (Brownian) motion of the purple membrane fractions in the liquid. This motion washes out the gratings. It is a reasonable value for the thermal motion of the membrane fractions in the liquid. The drop to a nonzero reflectivity value for a low λ_g can result from limited motion of the purple membrane fractions near the surfaces of the cell owing to viscosity.

In conclusion, we have conducted a study of the nonlinear absorption properties for two kinds of BR film. Our model of the levels by the rate equation was found to describe the experimental saturation behavior. Phase-conjugation experiments show the potential use of BR for image-processing purposes using low light intensities.

References

1. J. Y. Huang, Z. Chen, and A. Lewis, *J. Phys. Chem.* **93**, 3314 (1989).
2. Z. Chen, A. Lewis, H. Takei, and I. Nebenzahl, "Application of bacteriorhodopsin oriented in polyvinylalcohol films as an erasable optical storage medium," submitted to *Appl. Opt.*
3. E. Y. Korchemskaya, M. S. Soskin, and V. B. Taranenko, *Sov. J. Quantum Electron.* **17**, 450 (1987).
4. N. M. Burykin, E. Ya. Korchemskaya, M. S. Soskin, V. B. Taranenko, T. V. Dukova, and N. N. Vsevolodov, *Opt. Commun.* **54**, 68 (1985).
5. A. Lewis and V. Del Priore, *Phys. Today* **41**(1), 38 (1988).
6. G. Rayfield, *Phys. Bull.* **34**, 483 (1989).
7. R. R. Birge, C. F. Zhang, and A. L. Laurence, in *Proceedings of the Annual Meeting of the Fine Particle Society* (Fine Particle Society, Santa Clara, Calif., 1988).
8. C. Mobarry and A. Lewis, *Proc. Soc. Photo-Opt. Instrum. Eng.* **700**, 304 (1986).
9. M. Ottolenghi, *Adv. Photochem.* **270**, 29 (1980).
10. R. Korenstein and B. Hess, *Nature (London)* **270**, 184 (1977).
11. J. H. Hanamoto, P. Dupuis, and M. A. El-Sayed, *Proc. Natl. Acad. Sci. USA* **81**, 7083 (1984).